

# SOLITON SONIFICATION — EXPERIMENTS WITH THE KORTEWEG–DE VRIES EQUATION

*Rudolf Rabenstein*

Chair of Multimedia Communications and Signal Processing  
University Erlangen-Nuremberg  
Erlangen, Germany  
rabe@LNT.de

## ABSTRACT

Solitons are special solutions of certain nonlinear partial differential equations of mathematical physics. They exhibit properties that are partly similar to the solutions of the linear wave equation and partly similar to the behaviour of colliding particles. Their characteristic features are well-known in the mathematical literature but few closed-form solutions are available. This contribution derives algorithmic structures for the computation of solitons in a dimensionless space-time domain which can be scaled to the audio frequency range. The investigations are confined to first and second order solutions of the Korteweg-de Vries equation. Sound examples show that the effects of wave propagation and soliton interaction can be represented by audible events.

## 1. INTRODUCTION

Nonlinear methods for sound synthesis have been investigated since the days of analog modular synthesizers. It is not easy to classify the numerous approaches since nonlinear systems share no common property other than that the superposition principle of linear systems does not hold. Recent reviews of nonlinear sound synthesis methods can be found in a number of overview articles [1–3] and books [4, 5]. Nonlinear problems arise often from special applications. For example, in physical modelling the tension nonlinearities of strings and membranes have received considerable attention [6–8] while in virtual analog modelling, the nonlinearities of vacuum tube amplifiers are a topic of continuing interest [9–11]. Other approaches are encountered in formant synthesis [12], wind instruments [13], and in effects modelling [14] to name just a few.

This contribution discusses a class of nonlinear systems which – to the knowledge of the author – has so far not been subject of investigation for sound processing and synthesis. Nevertheless, it might be of interest here since special solutions of these nonlinear systems share properties with the propagation of waves in linear regimes, i.e. acoustical waves in air or the d’Alembert solution of vibrating strings. In contrast to the familiar oscillations of sound waves and of vibrating bodies, the wave-like behaviour is confined to solitary pulses. On the other hand, there are further effects without counterpart in linear systems which rather resemble the collision of nuclear particles like protons and neutrons. Both properties, the solitary wave character and the particle collisions, have contributed to the succinct name of these special solutions: *solitons*.

The existence of solitons is often explained as an interaction of dispersion and nonlinearity. In linear systems, the waveform of a propagating pulse is only preserved in the absence of dispersion. Otherwise, the waveform changes and short peaks typically

turn into broader ones with increasing width. On the other hand, dispersion-free nonlinear propagation media can have the opposite effect of sharpening a waveform. In acoustics, this effect leads to the creation of shock waves, e.g. in the bore of brass instruments at high pressure [5, 13]. In nonlinear and dispersive media both effects may balance each other and support stable solitary wave forms, called solitons.

Solitons are of technical interest in optical fibre communications [15], but they are not easily observed in acoustics. The formation of acoustic solitons has been reported for sound propagation in crystals with typical durations in the picosecond range [16], but there seem to be no physical systems which support solitons in the audio frequency range. Therefore, solitons are used here as a theoretical concept for devising synthesis algorithms rather than a physical model of a real-world sound source.

The problem of interest is here how to derive algorithmic structures for the computation of soliton-shaped solutions that are useful as waveforms for audio signals. The question is whether the properties of solitons (wave-like propagation and collision) have any auditory qualities that can be perceived by humans.

The benefit of such an attempt is an alternative to the usual graphical representation of solitons (see e.g. [17]). While images and movies show single solitons or isolated collisions of multiple solitons, a sound signal can convey the large scale character of soliton solutions with multiple collisions in a periodic or quasi-periodic fashion. In return, if soliton sounds turn out to be appealing then soliton sonification might be used as a sound synthesis method in its own right.

As a first step in this direction, this contribution reports some experiments with the Korteweg–de Vries equation which has been selected because its properties are well covered in the literature on applied mathematics. The results are presented in the following structure: Section 2 presents a short overview on solitons starting with a few historical remarks. The Korteweg–de Vries equation and its first and second order solutions are discussed in Section 3. The contributions of this paper start in Section 4 where generating structures are derived and further issues of soliton sonification are presented. An example is shown in Section 5.

## 2. SOLITONS

### 2.1. Historical Remarks

The story of the first observation of a soliton is retold in many publications on this topic. In short, John Scott Russel, a Scottish engineer observed a single non-periodic wave in a canal near Edinburgh in 1834. First he studied this effect in a self-built water

tank and ten years later he reported his observations to the British Association for the Advance of Science. His experimental findings were not well received until much later, when Boussinesq (1872) and Korteweg and de Vries (1895) set up equations for waves in shallow water.

Further advances were possible through the advent of digital computers. In the 1950s, Fermi, Past and Ulam performed computations in solid-state physics and observed also a balance between dispersive and nonlinear effects. In 1965, Kruskal and Zabusky undertook similar computations for the Korteweg–de Vries equation and introduced the term *soliton*. Stimulated by these numerical results, several research teams found mathematically rigorous solution strategies for the KdV equation, the nonlinear Schrödinger equation and a set of other nonlinear partial differential equations which exhibit solitons. Moreover the existence of solitons has been linked to other properties of mathematical physics like the validity of conservation laws and Hamiltonian systems.

A technical application evolved in fibre optics, where light pulses propagate according to the nonlinear Schrödinger equation. Here, solitons are used to carry bits of information along the fibre.

**Remark:** For details on this historical account see e.g. [18–22] and the literature cited there. Some of these sources contain an excerpt of Scott’s original report. Applications to fibre optics are presented e.g. in [15].

## 2.2. Literature on Solitons

The mathematical properties of solitons are covered not only in the original research papers but also in overview articles, in numerous books, and a growing number of web resources. The experiments with the KdV equation reported here are based on [18–26]. From these sources, [22, 26] contain nicely structured reference lists for further reading. Since Section 3 largely relies on these sources, no more detailed references will be given. Where appropriate, remarks with pointers to specific references are appended.

## 3. THE KORTEWEG–DE VRIES EQUATION

This section introduces one of the important nonlinear partial differential equations which exhibit soliton solutions, the *Korteweg–de Vries equation* or short the *KdV equation*. The presentation is confined to a few properties which are required for sonification. For a more complete treatment see the literature cited in Section 2.2.

### 3.1. Definition

The KdV equation describes a quantity  $u(x, t)$  which depends on a one-dimensional space variable  $x$  and on time  $t$ . From the various forms available in the literature, the following representation is adopted here

$$u_t + 6uu_x + u_{xxx} = 0, \quad -\infty < x < \infty, \quad 0 < t < \infty. \quad (1)$$

The subscripts  $x$  and  $t$  denote partial differentiation with respect to these variables and  $u = u(x, t)$  is used as a short notation.

It is the product  $uu_x$  which makes this equation nonlinear. Thus when  $u_1$  and  $u_2$  are two different solutions to (1), then in general  $u = a_1u_1 + a_2u_2$  is not a solution. However, when  $u_1$  and  $u_2$  tend to zero for  $x \rightarrow \pm\infty$  such that cross terms vanish,

then  $u = u_1 + u_2$  is also a solution. This case is important for solitons.

### 3.2. Scaling Symmetry

The non-applicability of the superposition principle does not mean lack of mathematical structure. Instead certain symmetries exist, e.g. the so-called *scaling symmetry*. It states that when  $u(x, t)$  is a solution to (1) then also  $\alpha^2 u(\alpha x, \alpha^3 t)$  is a solution, as can easily be shown by performing the space and time derivatives in (1).

The scaling symmetry allows to write the KdV equation for all kinds of physical problems in the normalized form of (1) by proper time, space, and amplitude scaling. Therefore this normalized form is used now for simplicity; the de-normalization to the audio rate is introduced when required.

### 3.3. First-Order Solitons

The KdV equation permits a multitude of different solutions. Only those are considered here which have approximately finite support, i.e. which vanish for  $x \rightarrow \pm\infty$ . For the most simple of these solutions an elementary derivation is given here which leads to solitons of the first order. Various explicit and tacit assumptions are made on the way without further justification. For example, any integration constants are set to zero.

#### 3.3.1. Derivation

The search for a solution to (1) is restricted to travelling wave solutions, i.e. to solutions of the form  $u(x, t) = \hat{u}(\xi(x, t))$  with  $\xi(x, t) = x - vt$  and  $u(x, t) > 0$ . The constant  $v$  represents the speed of a wave travelling in the direction of positive space and time. Performing the partial derivations in (1) leads to  $\hat{u}_t = -v\hat{u}_\xi$ ,  $\hat{u}_x = \hat{u}_\xi$ , and  $\hat{u}_{xxx} = \hat{u}_{\xi\xi\xi}$  such that

$$u_t + 6uu_x + u_{xxx} = -v\hat{u}_\xi + 6\hat{u}\hat{u}_\xi + \hat{u}_{\xi\xi\xi} = 0. \quad (2)$$

For the solution of (2) the following relations are used

$$\frac{1}{2} \frac{d}{d\xi} \hat{u}^2 = \hat{u}\hat{u}_\xi, \quad \frac{1}{3} \frac{d}{d\xi} \hat{u}^3 = \hat{u}^2 \hat{u}_\xi, \quad \frac{1}{2} \frac{d}{d\xi} (\hat{u}_\xi)^2 = \hat{u}_\xi \hat{u}_{\xi\xi}. \quad (3)$$

Integration of (2) leads to  $-v\hat{u} + 3\hat{u}^2 + \hat{u}_{\xi\xi} = 0$  and multiplication by  $\hat{u}_\xi$  and a further integration results in  $-\frac{v}{2}\hat{u}^2 + \hat{u}^3 + \frac{1}{2}\hat{u}_\xi^2 = 0$ .

Since the function  $u(x, t) = \hat{u}(\xi(x, t)) > 0$  is assumed to be positive, it can be replaced by the squared function  $\check{u}^2 = \hat{u}$  such that

$$-\frac{v}{2}\check{u}^4 + \check{u}^6 + 2\check{u}\check{u}_\xi^2 = -\frac{v}{2}\check{u}^2 \left[ \check{u}^2 - \frac{2}{v}\check{u}^4 - \frac{4}{v}\check{u}_\xi^2 \right] = 0. \quad (4)$$

Using the standard relations for hyperbolic functions

$$\operatorname{sech}^2 x + \tanh^2 x = 1 \quad \text{and} \quad \frac{d}{dx} \operatorname{sech} x = -\operatorname{sech} x \tanh x$$

it can be shown that the expression in brackets in (4) vanishes for

$$\check{u}(\xi) = \sqrt{\frac{v}{2}} \operatorname{sech} \left( \frac{\sqrt{v}}{2} \xi \right). \quad (5)$$

Thus the following hyperbolic function is solution to the KdV equation

$$u(x, t) = \hat{u}(x - vt) = \frac{v}{2} \operatorname{sech}^2 \left( \frac{1}{2} \sqrt{v} (x - vt) \right) \quad (6)$$

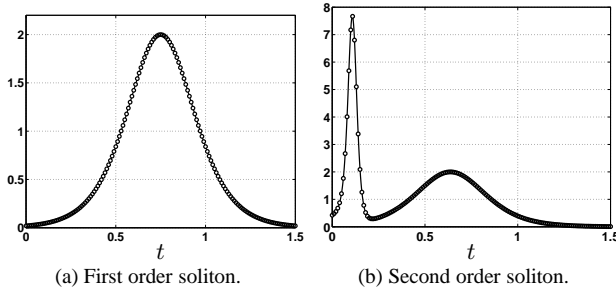


Figure 1: Solitons of first and second order. Solid lines: analytic solution, circles: values from the generating structures from Section 4.2.

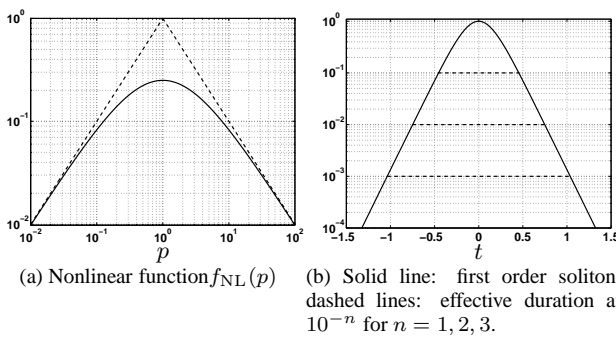


Figure 2: Nonlinear function  $f_{NL}$  and resulting first order soliton in logarithmic scale.

or equivalently with  $v = 4\kappa^2$

$$u(x, t) = 2\kappa^2 \operatorname{sech}^2(\kappa x - 4\kappa^3 t). \quad (7)$$

By derivation with respect to  $x$  and  $t$  it can be verified that  $u(x, t)$  actually solves (1) but the calculations are somewhat lengthy.

The general shape of  $u(x, t)$  for a fixed value of  $x$  as a function of time is shown in Fig. 1a). Obviously this solution is not periodic and goes to zero exponentially fast for  $t \rightarrow \pm\infty$ . It is called a soliton of first order and constitutes not only the most simple solution to the KdV equation but also a component of higher order solitons.

### 3.3.2. Effective Duration

The pulse-like shape of the first order soliton suggests to assign an effective duration in a similar fashion as a reverberation time is assigned to a room impulse response. Since the shape of the soliton does not change upon translation, the effective duration can be derived for

$$u_0(t) = u(0, t) = 2\kappa^2 \operatorname{sech}^2(4\kappa^3 t), \quad (8)$$

where the even symmetry of the sech-function has been used.

Now the effective duration  $t_D(n)$  is defined by normalizing  $u_0(t)$  to its maximum value

$$\left| \frac{u_0(t)}{u_0(0)} \right| \leq 10^{-n} \quad \text{for } t \geq \frac{1}{2}t_D(n). \quad (9)$$

For large  $t$ ,  $u_0(t)$  can be simplified to  $u_0(t) \approx 8\kappa^2 \exp(-8\kappa^3 t)$  such that the effective duration  $t_D(n)$  can be determined from

$$\frac{u_0(t_D(n)/2)}{u_0(0)} = 4 \exp(-4\kappa^3 t_D(n)) = 10^{-n} \quad (10)$$

as

$$t_D(n) = \frac{\ln 4 + n \ln 10}{4\kappa^3}. \quad (11)$$

Fig. 2b) shows the soliton from Fig. 1a) in logarithmic scale with the effective duration  $t_D(n)$  for  $n = 1, 2, 3$ .

## 3.4. Second Order Solitons

The discussion of second-order solitons starts with the case of higher order solitons and verifies the general case for first order solitons using the results from Section 3.3.1. Then the second order case is presented in some detail.

### 3.4.1. General Higher Order Solitons

The solution of the KdV equation which comprises higher order solitons is given by [18, 19]

$$u(x, t) = 2 \frac{\partial^2}{\partial x^2} \ln |\mathbf{M}(x, t)|, \quad (12)$$

where  $|\mathbf{M}|$  is the determinant of a square matrix. Its size determines the order of the solitons. A closed form formulation for  $\mathbf{M}$  can be found in [25, 26] as

$$\mathbf{M}(x, t) = \mathbf{I} + \int_x^\infty \exp(-\mathbf{A}x') \mathbf{b} \mathbf{c}^T \exp(-\mathbf{A}x') dx' \exp(8\mathbf{A}^3 t), \quad (13)$$

where  $\mathbf{A}$  and  $\mathbf{c}$  are given in terms of the parameters  $\kappa_i$  and  $c_i$  as

$$\mathbf{A} = \operatorname{diag}\{\kappa_1, \kappa_2, \dots\}, \quad \mathbf{b}^T = [1, 1, \dots], \quad \mathbf{c}^T = [c_1, c_2, \dots]. \quad (14)$$

This concise formulation is attractive as a general solution to a complex problem, but the occurrence of a matrix determinant and a double differentiation in (12) do not lead to an obvious discrete-time solution.

**Remark:** The parameters  $\kappa_i$  and  $c_i$  are the so-called scattering data for the reflectionless case, which generates solitons as solutions. The KdV equation has also other solutions which are not considered here. The term reflectionless has to be understood in the abstract sense of the inverse scattering theory, see e.g. [18, 19].

### 3.4.2. Verification of the First-Order Case

To gain some confidence in the general solution (12 - 14) it is now verified that it actually leads to the solution found in Section 3.3.1 when the matrix  $\mathbf{M}$  is of the size  $1 \times 1$ . In this case

$$\mathbf{M} = |\mathbf{M}| = 1 + c_1 \int_x^\infty e^{-2\kappa_1 x'} dx' e^{8\kappa_1^3 t} = 1 + q_1(x, t) \quad (15)$$

where  $q_1(x, t)$  results from the integration in (15) as

$$q_1(x, t) = \frac{c_1}{2\kappa_1} e^{-2\kappa_1 x + 8\kappa_1^3 t}. \quad (16)$$

The spatial derivatives of the determinant can be written as

$$d = |\mathbf{M}| = 1 + q_1, \quad d_x = 2\kappa_1 q_1, \quad d_{xx} = 4\kappa_1^2 q_1 \quad (17)$$

for the evaluation of (12)

$$u(x, t) = 2 \frac{\partial}{\partial x} \left( \frac{d_x}{d} \right) = 2 \frac{d d_{xx} - d_x^2}{d^2} = \frac{8\kappa_1^2}{\left( q_1^{\frac{1}{2}} + q_1^{-\frac{1}{2}} \right)^2}. \quad (18)$$

Now the solution (7) follows by inserting  $q_1$  from (16) and choosing  $c_1 = 2\kappa_1$ .

### 3.4.3. Second Order Case

The second order case follows from (12) with a matrix of size  $2 \times 2$  with the elements

$$M_{ij} = \delta_{ij} + \frac{c_j}{\kappa_i + \kappa_j} e^{-(\kappa_i + \kappa_j)x + 8\kappa_j^3 t} \quad i, j = 1, 2. \quad (19)$$

The calculation of the determinant leads to

$$d = 1 + q_1 + q_2 + K q_1 q_2 \quad \text{with} \quad K = \left( \frac{\kappa_1 - \kappa_2}{\kappa_1 + \kappa_2} \right)^2 \quad (20)$$

where  $q_1(x, t)$  and  $q_2(x, t)$  are defined as in (16). The derivatives are

$$d_x = -2(\kappa_1 q_1 + \kappa_2 q_2) + (\kappa_1 + \kappa_2) K q_1 q_2, \quad (21)$$

$$d_{xx} = 4(\kappa_1^2 q_1 + \kappa_2^2 q_2) + (\kappa_1 + \kappa_2)^2 K q_1 q_2. \quad (22)$$

After a lengthy evaluation similar to (18) the result can be written as

$$u(x, t) = 8 \frac{a_{10} q_2 + a_{01} q_1 + a_{11} + a_{21} q_1^{-1} + a_{12} q_2^{-1}}{\left( K(q_1 q_2)^{\frac{1}{2}} + q_1^{\frac{1}{2}} q_2^{-\frac{1}{2}} + q_1^{-\frac{1}{2}} q_2^{\frac{1}{2}} + (q_1 q_2)^{-\frac{1}{2}} \right)^2} \quad (23)$$

with the coefficients

$$a_{10} = \kappa_1^2 K, \quad a_{01} = \kappa_2^2 K, \quad a_{11} = 2(\kappa_1 + \kappa_2)^2 K, \quad a_{21} = \kappa_2^2, \quad a_{12} = \kappa_1^2. \quad (24)$$

As an example consider the values  $\kappa_1 = 1$ ,  $\kappa_2 = 2$  and  $c_1 = 6$ ,  $c_2 = 12$ . Inserting into  $q_1(x, t)$  and  $q_2(x, t)$  and grouping the exponential terms to hyperbolic functions as suggested by (23) leads to

$$u(x, t) = 12 \frac{\cosh(4x - 64t) + 4 \cosh(2x - 8t) + 3}{(\cosh(3x - 36t) + 3 \cosh(x - 28t))^2}. \quad (25)$$

An example for this second order solution is shown in Fig. 2b).

**Remark:** The result (23) for  $c_i = 2\kappa_i$  has been derived in [19, chapter 8.1] by Hirota's method; the special case (25) is also found in [19, chapter 4.5]. Note the sign change for  $u$  in [19] due to a different definition of the KdV equation.

### 3.4.4. Interaction of Second Order Solitons

The graphical representation of (25) in Fig. 1b) suggests that the second order solution is composed of two first order solitons as shown in Fig. 1a). A careful analysis shows that this is indeed the case, however the second order solution is not a simple linear superposition of two first order solutions.

An inspection of the components  $q_i$ ,  $i = 1, 2$  shows that their space time dependence has the form  $2\kappa_i x - 8\kappa_i^3 t = 2\kappa_i(x - v_i t)$ , i.e. they travel with the speed  $v_i = 4\kappa_i^2$ , where  $v_2 > v_1$  for  $\kappa_2 > \kappa_1$ . Therefore three different cases can be distinguished, where the terms slow and fast soliton refer to the speed  $v_i$ :

- The fast soliton lags behind the slow one, but approaches the slow one due its higher speed.
- The fast soliton has caught up with the slow one. Their interaction is also called a collision.
- The fast soliton has emerged from the collision and travels in front of the slow one.

The time regimes for these three cases can be identified by the effective duration from Section 3.3.2. Collision occurs when the difference between the positions of the maxima of  $q_1$  and  $q_2$  is less than the mean of their effective durations.

The effect that two components of a solution interact with each other and emerge from this interaction in their original shape is not at all common for nonlinear differential equations. It is a special feature for some of the nonlinear equations which support solitons. This feature can be shown for the second order solution of the KdV equation by a limit process, which is only roughly sketched here.

To this end the solution  $u(x, t)$  is represented in a spatial coordinate system which moves with either the speed  $v_1$  or  $v_2$ . Considering first only  $v_1$  then  $u(x, t)$  can be written as

$$u(x, t) = \hat{u}_1(\xi_1, t) \quad \text{with} \quad \xi_1(x, t) = x - v_1 t. \quad (26)$$

This change of variables is implemented in (23) by rewriting (16)

$$q_1(x, t) = \frac{c_1}{2\kappa_1} e^{-2\kappa_1(x - v_1 t)} = \frac{c_1}{2\kappa_1} e^{-2\kappa_1 \xi_1} = \hat{q}_{11}(\xi_1) \quad (27)$$

$$q_2(x, t) = \frac{c_2}{2\kappa_2} e^{-2\kappa_2 \xi_1} e^{2\kappa_2(v_2 - v_1)t} = \hat{q}_{21}(\xi_1, t) \quad (28)$$

with  $\hat{q}_{21}(\xi_1, t) \rightarrow 0$  for  $t \rightarrow -\infty$ ,

$$\hat{q}_{21}^{-1}(\xi_1, t) \rightarrow 0 \quad \text{for} \quad t \rightarrow \infty \quad \text{since} \quad v_2 - v_1 > 0.$$

Then the limit process  $\hat{u}_1^\pm(\xi_1) = \lim_{t \rightarrow \pm\infty} \hat{u}_1(\xi_1, t)$  is carried out such that  $x$  varies with  $t$  such that  $\xi_1(x, t) = \text{const.}$  After some calculations follows the result

$$u_1^\pm(x, t) = \hat{u}_1^\pm(\xi_1) = 2\kappa_1^2 \text{sech}^2(\kappa_1(x - v_1(t + t_1^\pm))). \quad (29)$$

Obviously, the solution  $u_1^+(x, t)$  after the collision has the same shape as  $u_1^-(x, t)$  before the collision, namely the shape of the first order soliton. The only remaining effect of the collision is a difference in time shift as indicated by  $t_1^\pm$ . This property is the typical property of a soliton solution.

The values for  $t_1^\pm$  are obtained by carrying out the limit process and are not reported here. Only their difference is of interest, since (29) allows to express  $u_1^+(x, t)$  in terms of  $u_1^-(x, t)$  as

$$u_1^+(x, t) = u_1^-(x, t - \Delta t_1) \quad \text{with} \quad \Delta t_1 = t_1^- - t_1^+ = \frac{1}{8\kappa_1^3} \ln \frac{1}{K}. \quad (30)$$

The same procedure is carried out for  $u(x, t) = \hat{u}_2(\xi_2, t)$  with  $\xi_2 = x - v_2 t$  and yields a similar result with a sign change for  $\Delta t_2$

$$u_2^+(x, t) = u_2^-(x, t + \Delta t_2) \quad \text{with} \quad \Delta t_2 = \frac{1}{8\kappa_2^3} \ln \frac{1}{K}. \quad (31)$$

For  $\kappa_2 > \kappa_1 > 0$ , both  $\Delta t_1$  and  $\Delta t_2$  are positive. Therefore the slow soliton with speed  $v_1$  emerges with a delay of  $\Delta t_1$  from the collision, while the fast soliton with speed  $v_2$  emerges advanced in time by  $\Delta t_2$ . During the collision, the solution  $u$  cannot be described by  $u_1^\pm$  and  $u_2^\pm$ , instead (23) has to be evaluated.

**Remark:** For  $\kappa_1 = 1$ ,  $\kappa_2 = 2$  and  $c_1 = 6$ ,  $c_2 = 12$  follows  $\Delta t_1 = \frac{1}{4} \ln 3$  and  $\Delta t_2 = \frac{1}{32} \ln 3$ . This case is presented in [19, chapter 4.5].

#### 4. SONIFICATION

The section above has reviewed some elements from soliton theory and has shown how to obtain functions which satisfy the KdV equation. Now the emphasis shifts from functions to signals. This section considers sonification and derives some generating structures which produces samples of solitons.

##### 4.1. General Approach

The waveforms shown in Fig. 1 are pulse-like and as such not immediately suitable for listening. Also the two-soliton interaction described in Section 3.4.4 is a non-repetitive effect and does not lend itself to the generation of audio signals. Therefore some kind of periodic or quasi-periodic recurrence has to be introduced in order to link the effects described above to audible events.

The sonification is achieved by letting the solitons travel along a circle with a large circumference such that the round trip time of the different components is large compared to the effective duration of the single solitons. The realization of this concept requires a detailed trigger mechanism to preserve the time shifts introduced by the soliton collisions.

###### 4.1.1. Introduction of Recurrent Behaviour

The general approach taken here is explained in Fig. 3. It shows the concept of a circular arrangement which resembles a particle collider. Solitons are injected at  $x = 0$  and travel along the  $x$ -axis according to their individual speed. Collisions may occur as the faster soliton catches up with the slower one. Depending on the circumference of the circle and the time delay resp. advance of the slower and faster soliton, collisions will occur repeatedly at different points of the circle. These collisions can be predicted from the delay and advance times calculated in Section 3.4.4. The signal picked up at  $x = x_p$  is then suitable for sonification.

**Remark:** The collider like structure in Fig. 3 has been inspired by the approach to spectral analysis in [20, Section IV].

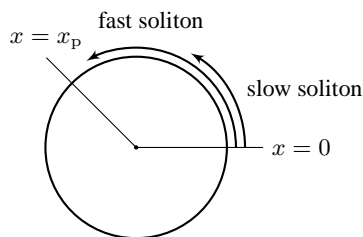


Figure 3: Concept of a circular arrangement for repeated soliton collisions.

###### 4.1.2. Computability

There are many good visualizations of solitons of low order available, e.g [17]. Usually they show the interaction of solitons for the

duration of the collision which is roughly given by the sum of the duration of the single solitons. The requirements for sonification are quite different because soliton-shaped signals have to be generated for seconds or possibly hours without a natural limit. The closed form equations (7) or (25) are of little use since the involved hyperbolic functions grow beyond all limits as time increases. This fact constitutes a potential source of trouble in numerical computations.

A first measure towards computability is to replace the exponential functions  $q_i(x, t)$  with their inverses

$$p_i(x, t) = q_i^{-1}(x, t) = \frac{2\kappa_i}{c_i} e^{2\kappa_i x - 8\kappa_i^3 t}, \quad i = 1, 2 \quad (32)$$

that tend to zero with time. Samples of  $p_i(x, t)$  can be easily generated by stable digital filters of first order as is shown now for first order solitons.

##### 4.2. Generating Structures

###### 4.2.1. First Order Solitons

To derive a generating structure for the first order soliton, rewrite (18) as

$$u(x, t) = 8\kappa_1^2 f_{NL}(p_1(x, t)) \quad (33)$$

with the memoryless nonlinear mapping

$$f_{NL}(p) = \left( p^{\frac{1}{2}} + p^{-\frac{1}{2}} \right)^{-2} = \frac{p}{(1+p)^2}. \quad (34)$$

The shape of  $f_{NL}(p)$  is shown in Fig. 2a). Since the argument  $p$  is exponentially decreasing, a logarithmic representation has been chosen.

To obtain a discrete-time sequence with samples of (18) fix the space at some position  $x = x_p$  and sample the time axis at  $t = kT$  with a suitable sampling instant  $T = f_s^{-1}$

$$u[k] = u(x_p, kT) = 8\kappa_1^2 f_{NL}(p_1[k]) \quad (35)$$

Since the nonlinear function  $f_{NL}(p)$  is memoryless, the sampling process has to be applied only to the exponential term  $p_1(x_p, t)$  as

$$p_1[k] = p_1(x_p, kT) = \frac{2\kappa_1}{c_1} e^{2\kappa_1 x_p} e^{-8\kappa_1^3 kT} = p_1[0] z_1^k, \quad (36)$$

$$p_1[0] = p_{10} = \frac{2\kappa_1}{c_1} e^{2\kappa_1 x_p}, \quad z_1 = e^{-8\kappa_1^3 T}. \quad (37)$$

The resulting algorithmic structure is shown in Fig. 4. The generation is triggered by a delta impulse, a most simple first order system generates samples of  $p_1$  which drive the nonlinear mapping. A multiplication with a constant gives the soliton-shaped signal.

The only approximation involved is that the generation does not start at minus infinity but at some time zero. If the time between the trigger and the maximum of the soliton is chosen sufficiently large, i.e. larger than the duration of the soliton, then this error can be made arbitrarily small. Fig. 1a) shows the analytic form according to (7) and samples produced by the structure from Fig. 4.

For first order solitons of the form (33) there are no collisions and their round trip time around the circle can be calculated directly from the circumference of the circle  $X$  as  $t_X = X/v$ . The signal  $\tilde{u}$  picked up at  $x = x_p$  is then

$$\tilde{u}(x_p, t) = \sum_{\mu=-\infty}^{\infty} u(x_p, t - \mu t_X) = 2v \sum_{\mu=-\infty}^{\infty} f_{NL}(p(x_p, t - \mu t_X)). \quad (38)$$

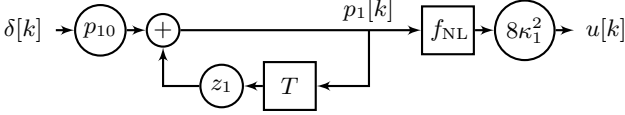


Figure 4: Generating structure for a soliton of first order.

Choosing the circle large enough such that the effective duration of the soliton is less than the round trip time  $t_D < t_X$  ensures that there is no overlap between both ends of the soliton pulse, i.e. there are no cross terms in  $f_{NL}$ . In this case superposition may be applied in good approximation and the observed signal can be written as

$$\tilde{u}(x_p, t) \approx 2v f_{NL} \left( \sum_{\mu=-\infty}^{\infty} p(x_p, t - \mu t_X) \right). \quad (39)$$

The discrete-time version can be easily generated with the structure from Fig. 4 when the impulse at the input is replaced by a periodic impulse train with spacing  $k_X = t_X/T$ .

Note that only the signals at one point  $x = x_p$  are generated. The circular movement is imitated by injecting new pulses at periodic time instances.

#### 4.2.2. Second Order Solitons

The generating structure for second order solitons can be derived directly from (23) by replacing  $q_i^{-1}$  by  $p_i$ . Different forms are possible by multiplying denominator and numerator by the same factor. One possibility is (40) which corresponds to the structure shown in Fig. 5

$$u(x, t) = 8 \frac{a_{10}p_1 + a_{01}p_2 + a_{11}p_1p_2 + a_{21}p_1^2p_2 + a_{12}p_1p_2^2}{(K + p_1 + p_2 + p_1p_2)^2}. \quad (40)$$

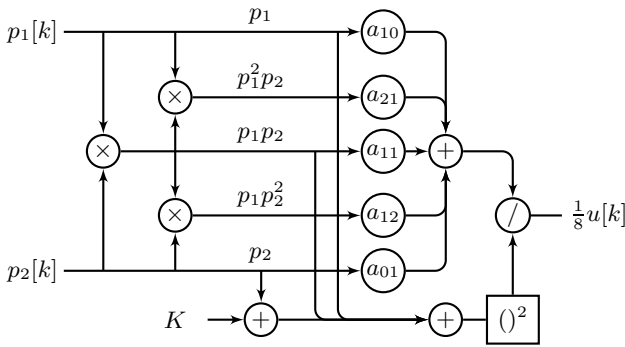


Figure 5: Generating structure for second order solitons.

The sequences  $p_1[k]$  and  $p_2[k]$  are generated from first order recursive digital filters as shown in Fig. 4. Then only three multiplications between these sequences are required for all necessary combinations of  $p_1$  and  $p_2$ . The remaining operations are multiplications with the constants in the numerator, computing the squared numerator and the final division. In comparison with Fig. 4, the diagram in Fig. 5 represents the two-input counterpart to the nonlinear function  $f_{NL}(p)$ .

Similar to Fig. 4, also the structure from Fig. 5 computes exact samples of the analytic waveform. Fig. 1b) shows an example of the collision period as obtained from the closed form equation (40) and the sequence  $u[k]$  computed according to Fig. 5.

But also first order solitons are generated correctly when only one input of Fig. 5 is nonzero. As an example set  $p_2 = 0$ ,  $x_p = 0$  and generate  $p_1$  from the left part of Fig. 4 with  $p_{10} = Kz_1^{-k_0}$  as  $p_1[k] = Kz_1^{k-k_0}$ . From Fig. 5 follows then

$$u[k] = 8 \frac{\kappa_1^2 K^2 z_1^{k-k_0}}{(K + Kz_1^{k-k_0})^2} = 2\kappa_1^2 \text{sech}^2(4\kappa_1^3(k-k_0)T). \quad (41)$$

as in (7) (and similar for  $p_2$  with  $p_1 = 0$ ). The delay by  $k_0$  is controlled via the multiplier  $p_{10}$ . This way, the soliton can be triggered well before it reaches its maximum at  $k = k_0$ . The generating structure from Fig. 5 can therefore be used for the non-collision and the collision case alike. It generates the correct first and second order solitons depending on the presence of the input signals  $p_1$  and  $p_2$ . Their correct trigger points are now discussed.

#### 4.3. Trigger Timing

Assume for a moment that there are two waves without interaction that can be treated according to linear superposition. When both start at  $t = 0$  with the respective speeds  $v_2 > v_1 > 0$  then they will meet again when the faster one is one full circle ahead of the slower one. This happens at time  $t_{lin}$  when  $v_2 t_{lin} = v_1 t_{lin} + X$  holds. The round trip time for the linear case is then

$$t_{lin} = \frac{X}{v_2 - v_1}. \quad (42)$$

Now return to the nonlinear case where two solitons collide at  $t = 0$  and  $x = 0$ . Then they emerge from the collisions with the time shifts  $u_1(x, t - \Delta t_1)$  and  $u_2(x, t + \Delta t_2)$  (see Section 3.4.4). The time  $t_0$  to and the location  $x_0$  of the next collision are then determined from  $v_2(t_0 + \Delta t_2) = v_1(t_0 - \Delta t_1) + X$  as

$$t_0 = t_{lin} - \frac{v_1 \Delta t_1 + v_2 \Delta t_2}{v_2 - v_1}, \quad (43)$$

$$x_0 = v_1(t_0 - \Delta t_1) = v_2(t_0 + \Delta t_2) \text{ modulo } X. \quad (44)$$

In a similar way follows that further collisions occur at multiples of  $x_0$  and  $t_0$ .

With the time between collisions known, a strategy for the second order case can be established. It uses the generating structure for second order solitons from Fig. 5 and a trigger mechanism for generating new solitons at the appropriate times. This strategy can be described as follows:

- In between two collisions, the slow soliton and the fast soliton are treated as separate pulses. They are generated by triggering only one input of Fig. 5 according to (41).
- When a collision occurs, but sufficiently far away from  $x_p$  then still the first order case can be applied as above. However when the next repetitions of the slow or the fast soliton are triggered then the time shifts  $\Delta t_1$  and  $\Delta t_2$  have to be considered.
- When a collision occurs in the vicinity of  $x_p$  then both inputs of Fig. 5 have to be triggered for the proper generation of the interaction during collision.

The procedure is shown in the top plot of Fig. 6. This plot represents a graphical timetable for motion of the solitons. The horizontal axis denotes time and the vertical axis denotes the position around the circle for a circumference  $X = 8\text{m}$  and with a pick up position at  $x_p = 0$ . Two collisions can be predicted from (43) and (44) starting with the first one at  $x = 0$  and  $t = 0$  (denoted by  $\circ$ ). Between the collisions, the solitons move like waves according to (6) (thin black lines). The approximate start and end as determined by the effective duration (11) is indicated by thick grey lines. The respective trigger points at  $x_p = 0$  can be read from the left grey line (denoted by  $\square$ ). Note that the trigger points can be predicted from Eqns. (6,11,43,44) without solving the KdV equation.

A single soliton event occurs when the next trigger time is outside of the duration of the current soliton. In this case, a slow or fast exponential is triggered for which the generating structure produces a single slow or fast soliton (see center and bottom of Fig. 6). The rising slope of the slow soliton is generated from values of  $p_1[k] > K$ , the maximum is reached for  $p_1[k] = K$  and for  $p_1[k] < K$  the slope falls again (similar for the fast soliton). The threshold of  $K$  is indicated by a horizontal line in the center plot of Fig. 6.

In the case of a collision near  $x_p$ , the two trigger points are so close that the second one falls into the duration of the first one (see Fig. 6 for  $t \approx 0.11\text{s}$ ). In this case also the second soliton is triggered together with the first one, i.e. earlier than in the single soliton case. The shift of the trigger point to an earlier instant is considered in a larger value of the multiplier, i.e. an additional delay. When both exponentials are active at the same time, the structure from Fig. 5 generates a second order soliton.

## 5. EXAMPLES

Two examples of soliton signals for the second order case generated according to the above strategy are shown in Fig. 7. The sample rate  $f_s$  has been chosen as 44.1 kHz and the duration of the resulting time signal is 1s. In both cases the slow component is the same with a value of  $\kappa_1 = 6$ . The signal on the top shows a fast component with  $\kappa_2 = 7.2$  while  $\kappa_2 = 14.4$  for the signal on the bottom. Both travel around the circle with regularly occurring collisions. Choosing different relations between the speeds  $v_1 = 4\kappa_1^2$  and  $v_2 = 4\kappa_2^2$  allows to change the characteristic of the sound. If both speeds are close together ( $v_2 < 1.1v_1$ ) then the sound is quasi-periodic with occasional beating like effects. When  $v_2 \approx 2v_1$ , then the sound resembles the hum of a large engine, with lots of small fluctuations. Sound samples are available at the website of the author [27].

## 6. CONCLUSIONS

This contribution has shown that first and second order solitons of the KdV equation can be synthesized by simple algorithmic structures. They consist mainly of first order digital filters to generate decaying exponentials and of a nonlinear function which produces the output signal. These experiments have to be regarded as preliminary and are more a proof of concept which leaves room for improvements and poses new questions. For example the trigger mechanism for the second order solitons could be solved more elegantly. Another challenge is the extension to solitons of third and higher order. The solution process presented here in a cursory fashion becomes rather tedious with higher orders. Finally it is of

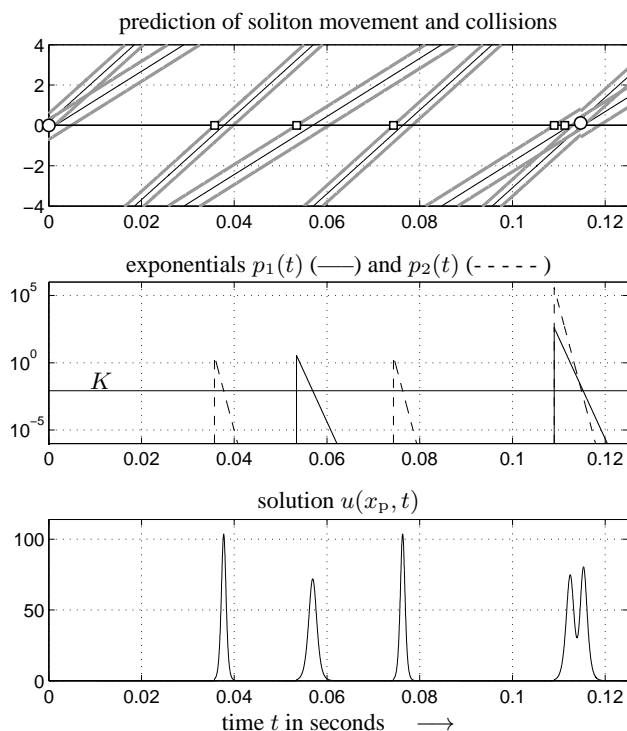


Figure 6: Workflow of soliton generation. Top: prediction of soliton movement and collisions from (43) and (44) with trigger points ( $\square$ ) and collisions ( $\circ$ ); center: exponential inputs  $p_1(t)$  and  $p_2(t)$ ; bottom: solitons generated according to Fig. 5.

interest to investigate also other nonlinear partial differential equations which support solitons. A promising candidate could be the nonlinear Schrödinger equation since it possesses solitons which travel in both directions.

**Acknowledgments.** Many thanks to Vesa Välimäki for pointing out relevant literature on nonlinear sound synthesis, to Parminder Singh for checking the calculations, and to Paolo Annibale for his help in proofreading the manuscript.

## 7. REFERENCES

- [1] Vesa Välimäki, Jyri Pakarinen, Cumhuri Erkut, and Matti Karjalainen, "Discrete-time modelling of musical instruments," *Reports on Progress in Physics*, vol. 69, no. 1, pp. 1–78, January 2006.
- [2] Victor Lazzarini, "Distortion synthesis," *Csound Journal*, vol. 11, 2009, <http://www.csounds.com/journal/>.
- [3] Jyri Pakarinen, Vesa Välimäki, Federico Fontana, Victor Lazzarini, and Jonathan S. Abel, "Recent advances in real-time musical effects, synthesis, and virtual analog models," *EURASIP Journal on Advances in Signal Processing*, 2011, Article ID 940784.
- [4] Julius O. Smith, *Physical Audio Signal Processing*, <http://ccrma.stanford.edu/~jos/pasp/>, accessed March 29, 2011, online book.

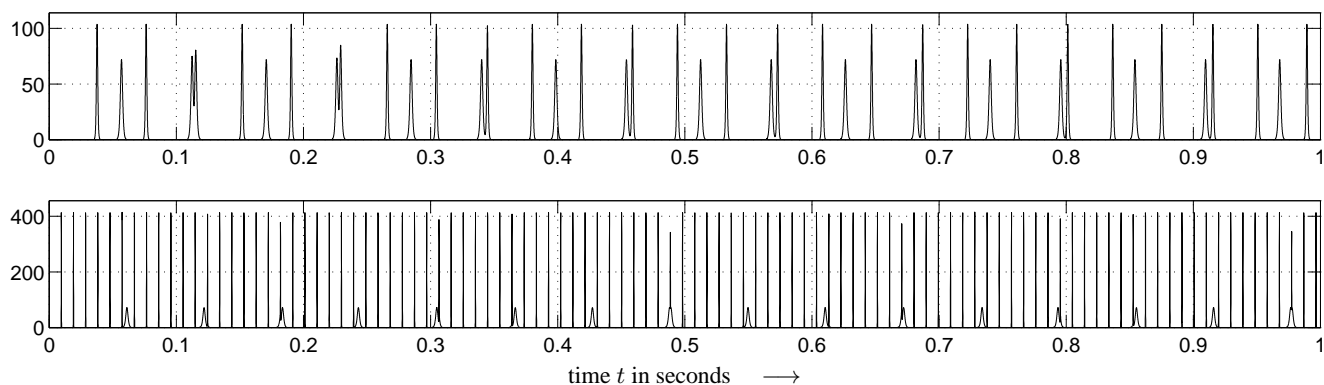


Figure 7: Sonification second order solitons of the KdV-equation for  $\kappa_1 = 6$  and  $\kappa_2 = 7.2$  (top) and for  $\kappa_1 = 6$  and  $\kappa_2 = 14.4$  (bottom).

- [5] Stefan Bilbao, *Numerical Sound Synthesis*, John Wiley & Sons, Chichester, UK, 2009.
- [6] T. Tolonen, V. Valimäki, and M. Karjalainen, “Modeling of tension modulation nonlinearity in plucked strings,” *IEEE Tr. on Speech and Audio Processing*, vol. 8, no. 3, pp. 300–310, May 2000.
- [7] Stefan Petrausch and Rudolf Rabenstein, “Tension modulated nonlinear 2D models for digital sound synthesis with the functional transformation method,” in *13th European Signal Processing Conference (EUSIPCO 2005)*, Antalya, Turkey, Sept. 2005.
- [8] Riccardo Marogna, Federico Avancini, and Balázs Bank, “Energy based synthesis of tension modulation in membranes,” in *Proc. Int. Conf. Digital Audio Effects (DAFx)*, Graz, Austria, 2010.
- [9] Jyri Pakarinen and David T. Yeh, “A review of digital techniques for modeling vacuum-tube guitar amplifiers,” *Computer Music Journal*, vol. 33, no. 2, pp. 85–100, Summer 2009.
- [10] Giovanni De Sanctis and Augusto Sarti, “Virtual analog modeling in the wave-digital domain,” *IEEE Transactions on Audio, Speech, and Language Processing*, vol. 18, no. 4, pp. 715–727, May 2010.
- [11] Jaromir Macak and Jiri Schimmel, “Real-time guitar preamp simulation using modified blockwise method and approximations,” *EURASIP Journal on Advances in Signal Processing*, 2011, Article ID 629309.
- [12] Miller Puckette, “Phase bashing for sample-based formant synthesis,” in *Proc. Int. Computer Music Conf. (ICMC)*, 2005.
- [13] Charles M. Cooper and Jonathan S. Abel, “Digital simulation of “brassiness” and amplitude-dependent propagation speed in wind instruments,” in *Proc. Int. Conf. Digital Audio Effects (DAFx)*, Graz, Austria, 2010.
- [14] Oliver Kröning, Kristjan Dempwolf, and Udo Zölzer, “Analysis and simulation of an analog guitar compressor,” in *Proc. Int. Conf. Digital Audio Effects (DAFx)*, Paris, France, 2011.
- [15] Govind P. Agrawal, *Nonlinear Fiber Optics*, Academic Press, 2nd edition, 1995.
- [16] H.Y. Hao, W. Singhsomroje, and H.J. Maris, “Studies of soliton formation of longitudinal acoustic phonons in crystalline solids,” *Physica B*, vol. 316-317, pp. 147–149, 2002.
- [17] Alex Kasman, “An introduction to solitons,” <http://kasmana.people.cofc.edu/SOLITONPICS/>, accessed April 12, 2012.
- [18] Alan C. Newell, *Solitons in Mathematics and Physics*, SIAM, Philadelphia, 1985.
- [19] P. G. Drazin and R. S. Johnson, *Solitons: an Introduction*, Cambridge texts in applied mathematics. Cambridge University Press, Cambridge, 1989.
- [20] Alwyn C. Scott, F. Y. F. Chu, and David W. McLaughlin, “The soliton: A new concept in applied science,” *Proceedings of the IEEE*, vol. 61, no. 10, pp. 1443–1483, October 1973.
- [21] Bonnie Kath and Bill Kath, “Making waves: Solitons and their optical applications,” *SIAM News*, vol. 31, no. 2, pp. 1–5, March 1998.
- [22] Peter Miller, “Course notes,” [http://math.arizona.edu/~mcl/MATH529\\_Spring08.html](http://math.arizona.edu/~mcl/MATH529_Spring08.html), 2008, acc. April 12, 2012.
- [23] William L. Kath, “Essentials of the inverse scattering transform,” <http://people.esam.northwestern.edu/~kath/431/istnotes.pdf>, 2011, Version 1.2, acc. April 12, 2012.
- [24] Spiro Karigiannis, “The inverse scattering transform and integrability of nonlinear evolution equations,” [www.math.uwaterloo.ca/~karigian/papers/ist.pdf](http://www.math.uwaterloo.ca/~karigian/papers/ist.pdf), June 1998, Minor Thesis, acc. April 12, 2012.
- [25] Tuncay Aktosun and Cornelis van der Mee, “Explicit solutions to the Korteweg–de Vries equation on the half line,” *Inverse Problems*, vol. 22, pp. 2165–2174, 2006.
- [26] Tuncay Aktosun, “Inverse scattering transform and the theory of solitons,” in *Encyclopedia of Complexity and Systems Science*, R. A. Meyer, Ed., pp. 4960–4971. Springer, New York, 2009, arXiv:0905.4746v1[nlin.Si] 28 May 2009.
- [27] “Authors home page,” <http://www.lms.lnt.de/research/activity/signale/synth/synth/>.